Influence of Thermal Ageing on Surface Degradation of Ethylene-Propylene-Diene Elastomer

R. Nevshupa,[1,2] L. Martínez,[1] L. Álvarez,[1] M. F. López,[1] Y. Huttel,[1] J. Méndez,[1] E. Román[1]

[1]*Instituto de Ciencia de Materiales de Madrid (ICMM-CSIC), c/Sor Juana Inés de la Cruz 3, Madrid 28049, Spain*
[2]*Fundación Tekniker, Av. Otaola 20, Eibar 20600, Spain*

Received 11 June 2009; accepted 27 March 2010
DOI 10.1002/app.32519
Published online 21 July 2010 in Wiley Online Library (wileyonlinelibrary.com).

ABSTRACT: Evolution of the surface characteristics of EPDM elastomer was studied as a function of thermal ageing at 80°C and 120°C in air for up to 100 days. The components of the surface free energy (SFE) were determined from contact angle measurements of five liquids using acid–base regression and Fowke's theories. SFE increased with ageing duration. For ageing at 80°C, SFE increased exponentially with time and stabilized after 60 days. Ageing at 120°C promoted a steep enhancement of SFE within the first 5 days followed by a slow long-term linear increase. Rate parameters of the SFE evolution were analyzed using Dakin's kinetic model. Analysis of the surface composition using X-ray photoemission spectroscopy evidenced an enhancement of the oxygen content with increasing the ageing time. The increase of the polar component of the SFE was attributed to the presence of these oxygen functional groups. This tendency was more pronounced for ageing at 80°C. © 2010 Wiley Periodicals, Inc. J Appl Polym Sci 119: 242–251, 2011

Key words: ageing; surfaces; XPS; surface free energy; rubber

INTRODUCTION

Ethylene-propylene-diene elastomer (EPDM) and other synthetic elastomers are widely used in various outdoor and industrial applications, especially in electrical insulation, pipes, and mounts. There is also rapidly growing use of EPDM in tribological applications, in automotive and transport engineering, e.g., for manufacturing bushing, gaskets, and inner liners,[1–4] due to its lightweight, low permeability, and higher stability as compared with conventional butadiene and isoprene rubbers.[5] However, even though this material presents a good performance, it is sensitive to oxidation at elevated temperatures. Oxidation of EPDM can produce degradation of its chemical, physico-mechanical, rheological, and surface properties. In tribological applications, there is a special concern in the quality of the elastomer surface since significant degradation of mechanical and tribological performance is usually associated with small changes in the surface composition and properties. Surface degradation of EPDM was studied recently by several groups using the artificial weathering test[3] and the thermal ageing tests.[5–8] Although most of these works are focused on chemical degradation studies, only a few of them deal with the study of the influence of weathering on variation of the surface free energy of EPDM.[3] Even less has been studied about the influence of thermal ageing on the surface free energy of EPDM. However, the lubrication performance, friction coefficient, and the rate of energy dissipation at friction contact may depend on the surface free energy. Therefore, the primary objective of this work is to study the effect of thermal ageing on the wettability and surface free energy of EPDM as function of ageing period and temperature. In addition, surface chemical composition of the samples is determined using X-ray photoemission spectroscopy (XPS) before and after thermal ageing to evaluate the correlation between the chemical modifications and surface free energy.

EXPERIMENTAL

Material and samples preparation

Commercial cured EPDM sheets (1 mm thick) were provided by Catelsa Hutchinson-Caceres, S.A. (Spain). The composition of EPDM is shown in Table I. Pieces of 10 × 10 mm^2 were cut from original sheets, then cleaned successively in acetone, ethanol, and distilled water using ultrasonic bath

Correspondence to: R. Nevshupa (rnevshupa@tekniker.es).
Contract grant sponsor: EU (Sixth Framework Program in the KRISTAL Project); contract grant number: 515837-2.
Contract grant sponsors: "Ramón y Cajal", "Juan de la Cierva", "Marie Curie"; contract grant numbers: MIF-CT-2006-22067, 980042.

TABLE I
Composition of the EPDM Elastomer Studied in this Work

Ingredients	phr[a]
EPDM	100
Carbon black	52.6
Paraffin oil	2.0
Antioxidants and process aids	3.7
Sulfur compounds	10.3

[a] Parts per hundred parts of rubber.

and finally dried in nitrogen gas. Thermal ageing was performed in a closed furnace at 80°C and 120°C in normal air atmosphere for different periods between 5 and 100 days. These ageing temperatures were selected considering the operating conditions in certain applications where the EPDM components must perform.

Contact angle measurements and determination of the components of surface free energy

Static contact angle (CA) measurements were carried out by a sessile drop method. The liquids used for the contact angle measurements were mili-Q distilled water, glycerol (99.5%), formamide (min. 99% GC), ethylene glycol (99%), and diiodomethane (99%), all liquids from Sigma-Aldrich Corp., St. Louis, MO. The surface energy components of these liquids are reported in Table II, in the order of decreasing polarity from the top to the bottom.[9,10] The surface energy evaluation system (SEE) equipped with a charge-couple device (CCD) was used for the drop image acquisition. This system also has a specific software for the contact angle analysis. Liquid drops of 4 μL were used in these measurements. Reproducibility of the CA values was verified by performing at least four measurements for each liquid and on each sample. Mean value and a standard error of mean were determined from the obtained data sets. All the measurements were performed at room temperature.

Mean CA values for five liquids were used for the surface free energy calculation of the EPDM samples. Several methods—Zisman, Fowke, Wu equation of state, Owens-Went, acid-base—can be used for this calculation according to the literature.[3,9,11–13] Because of different approaches used in these methods, the results may differ between methods.[2] In most of these commonly used methods only a limited number of liquids can be used for the surface free energy calculation and, therefore, the selection of different liquids can be a reason for the deviations in the final values obtained in different studies. In the acid–base regression method used in this work a large number of liquids can be used since the unknown parameters are determined by fitting the model equation to the experimental data. By doing so, the systematic errors can be reduced. In addition, the Fowke's model was used to determine the polar and dispersive components of surface energy to compare our results with the previously published data.

According to the acid–base model the total surface energy (γ^t) for non-metal materials can be calculated as a sum of two components: apolar Lifshitz—Van der Waals (γ^{LW}) and polar acid—base (γ^{AB}) component.[12] The polar component is a non-additive function of an electron acceptor, or Lewis acid, (γ^+) and an electron donor, or Lewis base, (γ^-) components:

$$\gamma^{AB} = 2\sqrt{\gamma^-\gamma^+} \tag{1}$$

The corresponding Young-Dupré equation for the interface of the *i*th liquid with an EPDM surface after the ageing time t_j is expressed by the following equation in terms of the polar and apolar components[12]:

$$\gamma_{Li}^t \frac{1+\cos(\theta_i(t_j))}{2} = \sqrt{\gamma_S^{LW}(t_j)\gamma_{Li}^{LW}} + \sqrt{\gamma_S^-(t_j)\gamma_{Li}^+} + \sqrt{\gamma_S^+(t_j)\gamma_{Li}^-}, \tag{2}$$

where the subscript *Li* denotes the *i*th liquid, the subscript *S* denotes the EPDM surface, and θ_i is the CA of the *i*th liquid with the EPDM surface. Parameters γ_{Li}^t, γ_{Li}^{LW}, γ_{Li}^+, and γ_{Li}^- are well-determined and published in the literature for each liquid, while three parameters of the EPDM surface: $\sqrt{\gamma_S^{LW}(t_j)}$, $\sqrt{\gamma_S^-(t_j)}$, and $\sqrt{\gamma_S^+(t_j)}$ are to be determined.

For each t_j, five equations of type (2) corresponding to five liquids used in our work form an overdetermined system of linear equations, which can be written in a matrix form:

$$\mathbf{Y} = \mathbf{Ab} \tag{3}$$

where **Y** is the matrix of independent variable [left side of eq. (2)], **A** is the ($n \times p$) matrix of known coefficients ($n = 5$, $p = 3$), and **b** is the matrix of unknown parameters:

TABLE II
Parameters of the Probe Liquids (mJ/m^2)

Liquid	γ^t	γ^{LW}	γ^{AB}	γ^-	γ^+
Water	72.80	21.80	51.00	25.50	25.50
Glycerol	64.00	34.00	30.00	57.40	3.92
Formamide	58.00	39.00	19.00	39.60	2.28
Ethylene glycol	48.00	29.00	19.00	30.10	3.00
Diiodomethane	50.80	50.80	0.00	0.00	0.00

$$\mathbf{Y} = \begin{bmatrix} \frac{(1+\cos(\theta_{11}))\gamma_{L1}^t}{2} & \cdot & \frac{(1+\cos(\theta_{1j}))\gamma_{L1}^t}{2} \\ \cdot & \cdot & \cdot \\ \cdot & \cdot & \cdot \\ \cdot & \cdot & \cdot \\ \frac{(1+\cos(\theta_{51}))\gamma_{L5}^t}{2} & \cdot & \frac{(1+\cos(\theta_{5j}))\gamma_{L5}^t}{2} \end{bmatrix} \quad (4a)$$

$$\mathbf{A} = \begin{bmatrix} \sqrt{\gamma_{L1}^{LW}} & \sqrt{\gamma_{L1}^{+}} & \sqrt{\gamma_{L1}^{-}} \\ \cdot & \cdot & \cdot \\ \cdot & \cdot & \cdot \\ \cdot & \cdot & \cdot \\ \sqrt{\gamma_{L5}^{LW}} & \sqrt{\gamma_{L5}^{+}} & \sqrt{\gamma_{L5}^{-}} \end{bmatrix} \quad (4b)$$

$$\mathbf{b} = \begin{bmatrix} \sqrt{\gamma_{S_1}^{LW}} & \cdot & \sqrt{\gamma_{S_j}^{LW}} \\ \sqrt{\gamma_{S_1}^{-}} & \cdot & \sqrt{\gamma_{S_j}^{-}} \\ \sqrt{\gamma_{S_1}^{+}} & \cdot & \sqrt{\gamma_{S_j}^{+}} \end{bmatrix} \quad (4c)$$

Each column in **Y** and **b**, identified with a subscript j, corresponds to one ageing period t_j. Mean values of the unknown parameters are determined from the matrix equation:

$$\mathbf{b} = (\mathbf{A}^t\mathbf{A})^{-1}\mathbf{A}^t\mathbf{Y} \quad (5)$$

and standard errors of the unknown parameters are found from the main diagonal of the covariance matrix:

$$\mathbf{K} = s^2(\mathbf{A}^t\mathbf{A})^{-1}, \quad (6)$$

where s^2 is the sample variance determined as:

$$s^2 = \frac{1}{n-p-1}(\mathbf{Y} - \mathbf{Ab})^t(\mathbf{Y} - \mathbf{Ab}). \quad (7)$$

In addition, the regression method was used to determine the polar and dispersive components of the surface energy according Fowke's theory, for which Young-Dupré equation can be written as follows:

$$\gamma_{Li}^{\mathrm{t}}\frac{1+\cos(\theta_i(t_j))}{2} = \sqrt{\gamma_S^{\mathrm{d}}(t_j)\gamma_{Li}^{\mathrm{d}}} + \sqrt{\gamma_S^{\mathrm{p}}(t_j)\gamma_{Li}^{\mathrm{p}}}, \quad (8)$$

where superscript d denotes a dispersive component and the superscript p denotes a polar component of the surface free energy. The matrix **A** and vector **b** for this model are the following:

$$\mathbf{A} = \begin{bmatrix} \sqrt{\gamma_{L1}^{\mathrm{d}}} & \sqrt{\gamma_{L1}^{\mathrm{p}}} \\ \cdot & \cdot \\ \cdot & \cdot \\ \cdot & \cdot \\ \sqrt{\gamma_{L5}^{\mathrm{d}}} & \sqrt{\gamma_{L5}^{\mathrm{p}}} \end{bmatrix}, \quad \mathbf{b} = \begin{bmatrix} \sqrt{\gamma_{S_1}^{\mathrm{d}}} & \cdot & \sqrt{\gamma_{S_j}^{\mathrm{d}}} \\ \sqrt{\gamma_{S_1}^{\mathrm{p}}} & \cdot & \sqrt{\gamma_{S_j}^{\mathrm{p}}} \end{bmatrix}. \quad (9)$$

Confocal microscopy

Surface microtexture of the EPDM samples before and after ageing was studied using white light confocal microscopy. The scan area was 1.30 × 0.95 mm^2 measured in 715 × 522 points equally spaced in each direction. The vertical scan step was 1 μm and the total scan distance in z direction was 60 μm. Roughness characteristics: Sa, Sq, and r of the EPDM samples, were determined from the 3D surface scans obtained. Sa is an arithmetical mean height of the surface, Sq is a root mean square height of the surface, and r is the roughness ratio defined as the ratio of true area of the solid surface to the apparent (projected) area. The first two parameters were determined according to the standard procedure,[14] while the last one was calculated according to the method described in the Appendix.

Surface characterization by x-ray photoemission spectroscopy

The XPS measurements were carried out using a Phoibos 100 ESCA/Auger spectrometer with a nonmonochromatized MgK_α (1253.6 eV) X-ray source. Wide energy range spectra and narrow energy range spectra were obtained. The wide scans provide complete information on the chemical composition of the sample surface while the narrow scans provide more detailed information on specific elements and chemical bonds. The wide scans were recorded with an energy step of 0.25 eV and a pass energy of 40 eV. The narrow scans of the C 1s core level were recorded with an energy step of 0.1 eV and a pass energy of 15 eV. Before the analysis of the XPS spectra, the contribution of the MgK_α satellite lines were removed, and the spectra were subjected to a Shirley background subtraction formalism.[5] The binding energy (BE) scale was calibrated with respect to the C 1s peak at 285 eV.[15,16]

RESULTS AND DISCUSSION

Confocal microscopy

The surface images of EPDM elastomer after different ageing times at 80°C and 120°C show that some changes of the surface microtexture occurred during ageing. Figure 1 shows the reconstructed pseudo 3D images of the samples aged at 120°C for different ageing periods, where the changes observed were more significant. At the beginning of ageing, the surface had some regular microtexture in a form of parallel grooves resulting from the molding process. During ageing, this microtexture progressively vanished and completely disappeared after 20 days of ageing. Starting from approximately a 10 days ageing period a new microtexture mode characterized

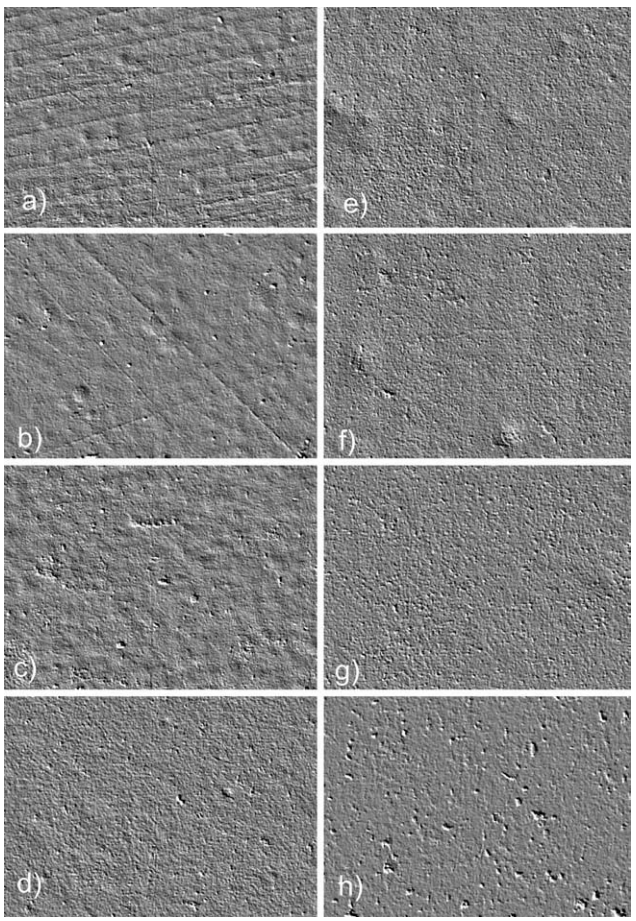

Figure 1 Pseudo 3D images of the EPDM surface reconstructed from the surface scans using white light confocal microscopy. (a) Before ageing and after (b) 5 days, (c) 10 days, (d) 20 days, (e) 30 days, (f) 60 days, (g) 80 days, and (h) 100 days of ageing. The size of each image is 1.30 $\times$ 0.95 mm^2.

by small protruding islands appeared. The size of these islands grew up with the ageing time, while the surface density of these islands decreased. Delor-Jestin et al.[17] observed appearance and migration of surface products after storing and weathering tests of EPDM, however, in their experiments the surface residues quickly vanished after heating at 100°C and 150°C. In contrast, in our work, the surface microtexture appeared during heating and was not affected by the samples cleaning in acetone, ethanol, and distilled water.

Various characteristic parameters of the roughness extracted from these scans are shown in Table III. The roughness parameters increased almost linearly with time during ageing. Although, Sa and Sq increased three- to four-fold, the increase of the roughness ratio was very small, about 5.6% of its initial value.

Contact angle measurements

Figure 2 shows the evolution in time of the experimentally measured mean contact angles (CA) of five liquids on the EPDM samples aged at 80°C (a) and 120°C (b). At the beginning, there was a steep decrease of the CAs for all liquids. This decrease was larger at 120°C than at 80°C. At the higher temperature, the first decrease of the CA occurred during the first 5 days of ageing [shown by dash lines on Fig. 2(b)], while at the lower temperature it lasted for 30 days, and then CAs stabilized.

Experimental data for 80°C were fitted by an exponential decay function:

$$\theta = \theta_1 + \alpha \exp(-t_a/t_1), \tag{10}$$

where θ is CA for a liquid, t_a is the ageing period, and the parameters θ_1, α, and t_1 have to be found from the fitting. These parameters have the following physical meanings: θ_1 is the steady value of CA at $t_a \to \infty$, $\theta_1 + \alpha = \theta_0$ is the initial value of CA, t_1 is the time constant of decay. Function (10) corresponds to the solution of Dakin's model of thermally activated degradation of polymeric materials during ageing[8]:

$$-\frac{d\varepsilon}{dt_a} = \nu \exp\left(-\frac{E_a}{RT}\right) f(\varepsilon), \tag{11}$$

where ν is the pre-exponential factor, E_a is the activation energy, R is the universal gas constant, T is the temperature, ε is the extent of reaction (in our case is CA), and $f(\varepsilon)$ is a function of the extent. In our model we used a simple first-order function $f(\theta) = \theta - \theta_0$.

Equation (10) fits the experimental data quite well as can be observed from the normal distribution of residuals and high values of the coefficients of determination ranged between 0.5 and 0.94. Mean value of the time constant with corresponding standard error for five liquids is $t_1^{80} = 13.1 \pm 7.8$ days. Standard deviation for the approximation curves is shown

TABLE III
Roughness Characteristics of EPDM Samples Aged at 120°C

Ageing, days	0	5	10	20	30	60	80	100
Sa (μm)	0.337	0.458	0.409	0.585	0.925	0.629	0.727	0.986
Sq (μm)	0.456	0.687	0.533	0.774	1.310	0.876	0.976	1.850
r	1.0038	1.0068	1.0041	1.0163	1.0145	1.0135	1.0337	1.0600

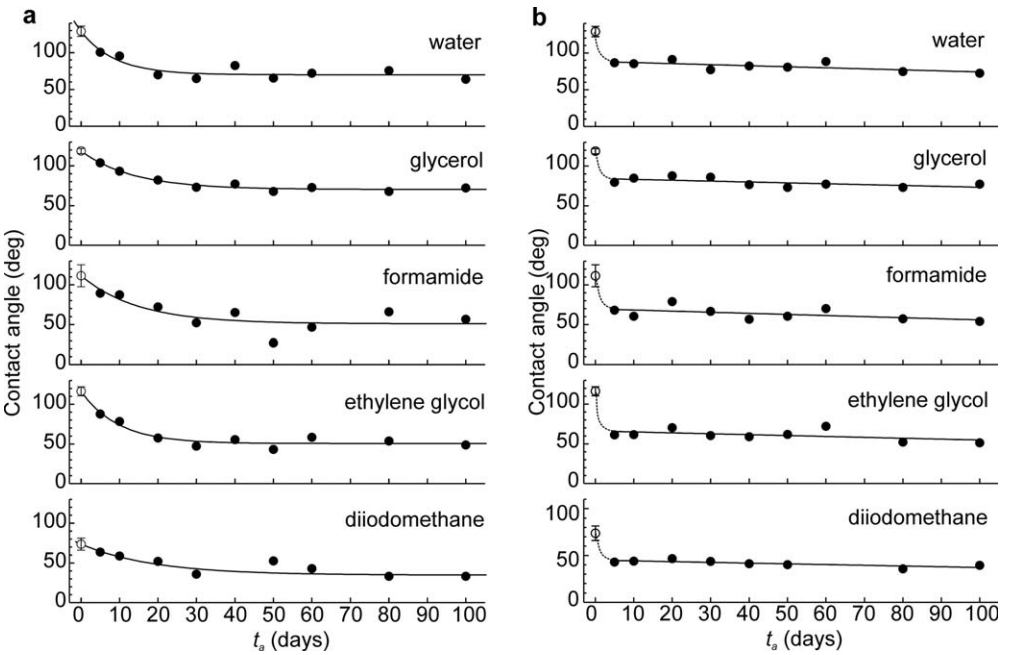

Figure 2 Evolution of the CAs on EPDM as function of ageing time at (a) 80°C and (b) 120°C. Circles—experimental data, solid lines—approximation by exponential function (a) and linear function (b).

in Figure 2 by a vertical bar on the left side of the plots.

For 120°C, the initial decay was very fast and, therefore, fitting of the experimental data using eq. (10) could not be performed with satisfactory goodness of approximation. From the experimental data, we estimated the time constant of this decay to be $t_1^{120} \leq 1$ day. In general, the results indicate that the thermal treatment favored the hydrophilic character of the samples.

The model of eq. (10) predicts that after a characteristic ageing time $t_a^c \approx 5t_1$ the decay is completed by 99% and the reaction extent stabilizes. However, in this work we observed a long-term slow decay of the CA, which continued after the characteristic ageing time. This long-term decay was found for all liquids. For ageing at 120°C, this long-term decay was almost linear. For the samples aged at 80°C, the decay was similar, but with lower rate. The rates of the long-term decay were determined from the slopes of linear functions fitted to the right part of the plots CA versus t_a. The results of the fitting are shown in Table IV, and the linear functions are plotted in Figure 2(b) with solid lines. The decay rates as well as the absolute CA values decreased with decreasing the liquid polarity from water to diiodomethane. The long-term decay rates were normalized to the value $\theta_i|_{t_a=100}$ and then plotted in Figure 3. Mean values and standard errors of mean (se) for S_r are included in this figure by dashed lines. For

TABLE IV
Long-Term Slopes and Standard Error of Mean (se) (deg/day)

	80°C		120°C	
Liquid	Slope	se	Slope	se
Water	−0.034	0.107	−0.140	0.050
Glycerol	−0.051	0.064	−0.110	0.050
Formamide	−0.130	0.270	−0.139	0.079
Ethylene glycol	−0.034	0.090	−0.113	0.070
Diiodomethane	−0.135	0.158	−0.078	0.025

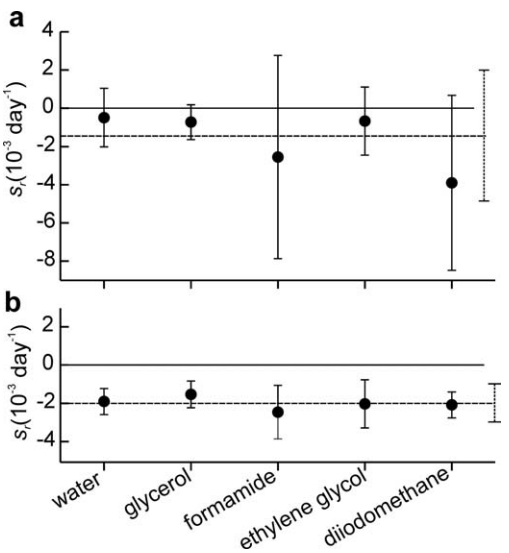

Figure 3 Long-term decay rates of the CAs on EPDM aged at (a) 80°C and (b) 120°C normalized to $\theta_i|_{t_a=100}$.

80°C, there is a large variance of the determined decay rates, which impedes any further analysis of these data. For the ageing temperature 120°C, the values of the normalized decay rates, S_r, are close one to another and statistically significant. This indicates that the decay rate is proportional to the absolute value of the CA and not to the difference $\theta - \theta_0$ as predicted by the model (10). The possible reasons for the discrepancy between the model and the experimental data will be discussed later.

As CA depends not only on the surface chemistry but also on the surface roughness, intrinsic CA, i.e., the contact angle of the same liquid on an ideally smooth surface of the same material, was determined before calculation of the surface free energy. Homogeneous wetting regime of a liquid on a rough surface is described by the following equation of the Wenzel model[18,19]:

$$\cos \theta_a = r \cos \theta, \tag{12}$$

where θ_a is the experimentally measured CA (hereafter apparent CA) corresponding to the stable equilibrium state of a liquid drop on a rough homogeneous surface, θ is the Young CA (intrinsic), r is the roughness ratio.

The most significant differences between the experimentally measured (apparent) CA and calculated Young CA were found for diiodomethane and ethylene glycol and only for the ageing periods of 100 and 80 days. The maximum difference was 3.8°. For other measurements, especially for the ageing periods from 0 to 60 days, the difference was below 1°. All differences were statistically insignificant as compared with the uncertainties of the CA measurements.* In addition, the slopes of the long-term decay were calculated for the apparent CA. For all liquids, the differences between the slopes determined for the apparent CA and Young CA were statistically insignificant. These results definitely rule out the influence of the surface microstructure on the behavior of the surface free energy during ageing.

Resuming, the influence of the microtexture variation on wettability during ageing up to 100 days was negligible for the polar liquids. The liquids with the highest polarity have larger CA for all ageing times. Consequently, the decrease in the polarity of the liquids results in smaller CA, especially for long ageing periods. Therefore, the evolution of the CA should be related to different mechanisms of EPDM degradation, probably to the change of the surface chemical composition.

*Determined using t-test at significance level $\alpha = 0.05$ and the number of degrees of freedom $n = 3$.

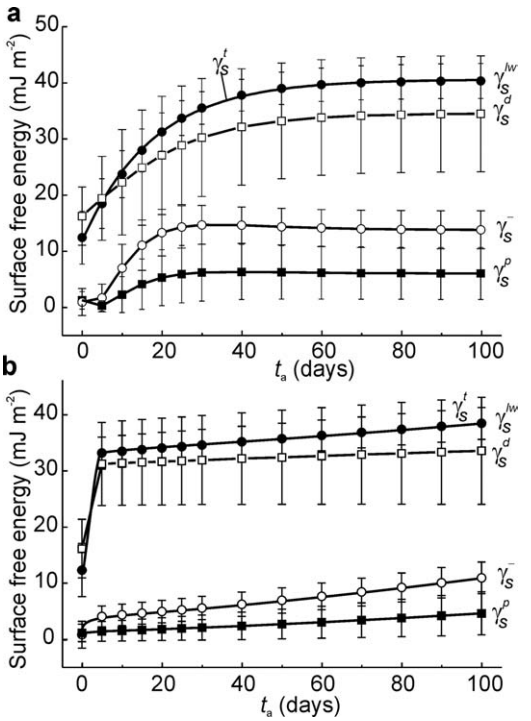

Figure 4 Evolution of the surface free energy of EPDM as a function of the ageing time at (a) 80°C and (b) 120°C.

Determination of the surface free energy

The components of the surface free energy of the elastomer as function of the ageing period determined using acid–base regression method [eqs. (4)–(6)] are shown in Figure 4(a,b), for 80°C and 120°C, respectively. For both temperatures, the component γ^+ was statistically insignificant. Therefore, this term was omitted and the calculation was repeated to determine the components γ_S^{LW} and γ_S^- more accurately. Filled and opened circles in Figure 4 represent γ_S^{LW}, and γ_S^-, respectively, as function of ageing time. As the component γ^+ is neglected, EPDM surface is mainly γ_S^- monopolar. In the absence of a parameter of the opposite sign, energy parameters of a monopolar surface do not contribute to the total surface energy (energy of cohesion) since the polar component $\gamma_S^{AB} = 0$.[12] Therefore, the total surface energy $\gamma_S^t = \gamma_S^{LW}$ [see eq. (1)]. However, monopolar surfaces can strongly interact with bipolar liquids.

At the lower temperature, γ_S^{LW} increased exponentially with ageing period reaching almost stable values after 60 days of ageing. Parameter γ_S^- had an induction period of $\sim$ 5 days ($\sim$ 120 h). These results agree with the previous works in which the induction period during thermal oxidation of EPDM was 130 h at 80°C[6] and 150 h at 150°C.[16] Variation of the induction periods in different works can be due to the differences in the EPDM composition, more

specifically, in the content of carbon black and antioxidants.[17,19] After induction, γ_S^- increased rapidly until reaching the maximum in 30 days. Then, it remained almost constant with a slightly decreasing tendency, which, however, was within a standard error. The solid line connecting the filled circles in Figure 4(a) is an approximation of the experimental data by an exponential function with a time constant of 17.7 ± 0.4 days, which is consistent with the time constant of the CA exponential decay.

For 120°C [Fig. 4(b)], there was a steep increase of γ_S^{LW} at the beginning of ageing. Then, γ_S^{LW} increased almost linearly with ageing time but with lower rate than at the beginning of ageing. After 100 days ageing period at 120°C, γ_S^{LW} was ~ 5% smaller than at 80°C, but maintained the linear growth. However, at 80°C γ_S^{LW} was at its steady value.

Evolution of γ_S^- is similar to that of γ_S^{LW}, but the initial increase of γ_S^- was not as steep as for γ_S^{LW}. At the beginning of ageing at 120°C, γ_S^- was notably smaller than at 80°C. This difference vanished only at large ageing periods. At 120°C, the induction period was not observed. This could be explained by shortening of the induction period with temperature. Indeed, for pure EPDM at 120°C the reported induction period is only 10 h[6] that is much smaller than the smallest ageing period used in this work.

In addition to the acid–base method, we determined the polar and dispersive components according with the Fowke's theory. The results are shown in Figure 4 by open and filled squares for γ_S^d and γ_S^p, respectively. The γ_s^t determined as a sum of these two components coincides with the value obtained by the acid–base method. In general, the behavior of γ_S^d was similar to that of γ_S^{LW} and the behavior of γ_S^p was similar to that of γ_S^-, but the absolute values of γ_S^d and γ_S^p were correspondingly lower than of γ_S^{LW} and γ_S^-.

The initial value of γ_s^t is consistent with the data of Zhao et al.[3] for EPDM before weathering test. In their weathering test at ambient temperature,[3] γ_s^t first increased and then stabilized at 23.8–25.4 mJ/m^2. These values are almost two-fold smaller than in our thermal ageing experiments. This fact supports a hypothesis of a thermally activated nature of the processes responsible for the increase of the surface energy. The γ_S^d values in thermal ageing and weathering tests were similar.

Two main processes occur in the EPDM during ageing: (i) crosslinking, which begins from the start of the thermal exposure of EPDM and (ii) oxidation of the elastomer chains. Kumar et al.[6] reported the characteristic times of the crosslinking for EPDM at 80°C and 120°C are 100 h and 12.5 h, respectively. After these periods, the material is considered fully crosslinked. These times are much shorter than the periods of initial transitional increase of the dispersive and apolar components of surface free energy at corresponding temperatures in our experiments. Thus, crosslinking hardly can explain the long-term behavior of these SFE components. In contrast, the oxidation process resides in chain scission and recombination accompanied by formation of oxygen functional groups and radicals, which may lead to significant change of the surface free energy.[3]

XPS measurements

For better understanding, the influence of the oxidation on the surface free energy of EPDM, some samples were analyzed using XPS. More specifically, the evolution of the surface chemical composition of the samples aged at 80°C for various periods was measured. In addition, the samples aged at 80°C and 120°C during 100 days were also compared to provide insight into the effect of the ageing temperature on the surface chemical composition. Table V summarizes the chemical composition (%$_{at}$) obtained from the analysis of the wide energy range scan of the selected samples after thermal ageing experiments, where an as received sample was included for comparison purposes. Carbon was the main element in the spectra due to the backbone structure of the polymer. Oxygen in the spectra of EPDM is generally attributed to curing reactions and presence of ZnO. Other elements like nitrogen, silicon, or zinc were also found in smaller amounts due to the additives included in the elastomer during the fabrication process. As XPS is a superficial analysis technique, the variation of these elements present in small amounts on the surface could be related to diffusion processes during ageing and segregation of the impurities on the surface.

A continuous increase in the oxygen content with the ageing time was registered on the ageing process at 80°C. This evolution is evident from the continuous decrease of the ratio C/O ratio calculated for each case (last column). In addition, for both temperatures there was certain increase of nitrogen and silicon concentrations for the 100 days ageing. This effect could be related to migration of additives towards the surface. Being thermally activated process, migration of additives should be faster at

TABLE V
Chemical Composition Obtained by XPS of Some EPDM Samples After Thermal Ageing

Thermal ageing		Composition (%$_{at}$)					
T (°C)	t_a (days)	C	O	N	Si	Zn	C/O ratio
As received		93	5	0	2	Traces	19
80	5	90	7	0	2	1	13
80	50	88	9	1	1	1	10
80	100	82	14	3	1	Traces	6
120	100	80	13	2	4	1	6

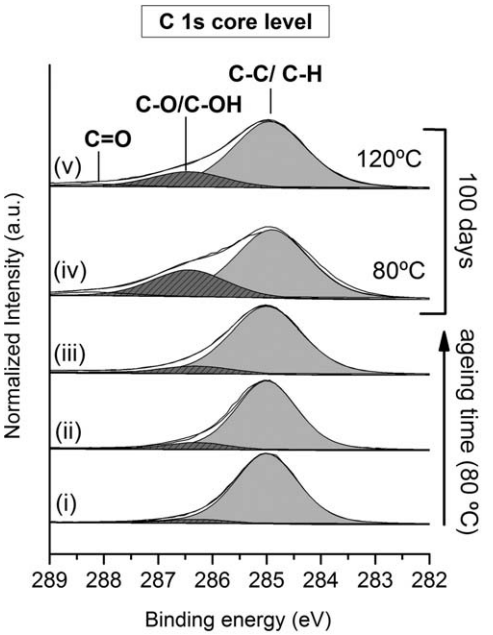

Figure 5 C 1s spectra of EPDM (i) as received and aged, (ii) 5 days at 80°C, (iii) 50 days at 80°C, (iv) 100 days at 80°C, and (v) 100 days at 120°C.

higher temperatures as shown in Table V, where Si concentration is higher at 120°C than at 80°C.

To investigate changes in the carbon bonding of the EPDM samples, a curve fitting procedure of the C 1s core level spectrum was performed for each sample. The results are shown in Figure 5. The broad carbon peak observed in the binding energy range from 283 eV to 289 eV can be attributed to different carbon-based surface functional groups at different binding energies. The carbon 1s peak was fitted with four gaussian/lorenzian components with the maximum intensity at binding energies of 285 eV, 286.3 eV, 288.1 eV, and 289 eV. In agreement with the literature, these different binding energies were assigned to C—C or C—H at 285 eV, hydroxyl (C—O/C—OH) at 286.3 eV, carbonyl (C=O) at 288.1 eV and carboxyl (O—C=O) at 289.0 eV.[6] Most part of the carbon is in the form of C—C/C—H. From the analysis of the samples treated at 80°C for different ageing periods, it can be observed that as the ageing period increased, the amount of carbon atoms bonded to oxygen atoms, especially hydroxyl, also increased. This effect is similar to the evolution of the oxygen content registered in the wide energy range scan (Table V). Such behavior was previously observed by Zhao et al.[3] and Delor-Jestin et al.[17] After 100 days at 80°C, these carbon–oxygen bonds were mainly in form of hydroxyl (20%), followed by a small proportion of carbonyl (4%) and traces of carboxyl (1%). The comparison of the C 1s core level analysis of the samples treated at 80°C and 120°C for 100 days reflected that, despite the fact that EPDM presented a similar amount of oxygen on its surface after both treatments (Table V), the proportion of oxygen functional groups at a higher temperature was lower. According to Zhao et al.,[3] C—OH bonds in the C 1s core level peak is the main ageing product of EPDM. However, the results obtained suggested that treatments above 100°C could cause hydroxyl desorption and, therefore, could explain the lower C—O content registered after the treatment at higher temperature. This effect, probably, corresponds to the decrease of γ_S^- component after 30 days ageing at 120°C.

Long-term behavior of SFE

The behavior of surface free energy is characterized by two modes: (a) exponential growth corresponding to a first-order thermally activated reaction of type (11) and (b) linear growth. Budrugeac and Segal[8] determined the activation energy for thermal degradation of EPDM between 13.9 and 20 kcal/mol depending on the reaction extent. The approximate values of the activation energy for the exponential SFE growth [(a)-mode] in our work determined from the time constants at 80°C and 120°C using (11) are considerably higher than in their work[8]: 63.5–83.7 kJ/mol. The values obtained in our work are close to the activation energy of oxidation of heavy fuel oil determined by Ayala et al.[20] (67 kJ/mol) but much lower than the oxidation activation energy of EPDM during induction period: 146.4–171.4 kJ/mol.[21] Thus, mode (a) most likely should be attributed to normal oxidation of EPDM.

Mode (b) does not correspond to the first-order thermal activation model and can be due to several reasons: (i) reaction of different order, (ii) non-constant activation energy, and (iii) existence of two or more processes with different kinetics.

For logarithmic dependence $E_a(\varepsilon)$, the kinetic equation of the reaction is:

$$-\frac{d\varepsilon}{dt_a} = \nu\varepsilon^{n+1}, \tag{13}$$

i.e., reaction rate is a power function of the reaction extent. This equation has the following solution ($n \neq 0$) [8]:

$$\varepsilon = (n\nu t + C^{-n})^{-\frac{1}{n}}, \tag{14}$$

where C is the integration constant found from initial conditions. For negative n corresponding to the reaction order below unity, the reaction extent increases with time, while the rate of the increase depends on the parameters in (13). For $n = -1$, EPDM degradation is a zero-order reaction and reaction extent increases linearly with time, as in the case of thermal ageing at 120°C. This result is

consistent with findings of Zhao et al.,[3] who reported that in artificial weathering conditions, the surface degradation of EPDM is a zero-order reaction. Hence, variable activation energy can explain mode (b) of the long-term evolution of the surface free energy. More extensive study is necessary for more detailed quantitative analysis of the mechanisms of the EPDM surface degradation at long-term scale.

CONCLUSIONS

Samples of EPDM were thermally aged for different periods up to 100 days by heating at 80°C and 120°C. Surface free energy, surface morphology, chemical composition, as well as carbon bonds were studied as a function of ageing treatment.

The contact angles of all liquids measured presented an exponential decay with time in both ageing treatments although was more pronounced for the ageing at 120°C. Both ageing treatments in air at 80°C and 120°C presented an increase of the total surface free energy with the ageing time, although the evolution in both cases was different. The ageing at 80°C produced an exponential increase of the surface free energy that stabilized after 60 days. In this treatment, an induction of γ_S^- was registered for the first 5 days. On the other hand, the ageing at 120°C presented a sharp increase in the surface free energy at low ageing periods and, then, increased linearly with ageing period without reaching a steady value as it occurred in the ageing at 80°C.

Surface chemical analysis revealed an increase of the oxygen content and the formation of oxygen functional groups, mainly as hydroxyl. The presence of these groups was more pronounced after the treatment at 80°C than at 120°C. These chemical modifications are probably the cause for the evolution observed on the surface free energy, as the evaluation of the surface morphology with the treatment time does not justify the tendency observed in the CA or the surface free energy.

In resume, not only the characteristic times for crosslinking are different at both temperatures but also the ageing process itself. Higher ageing temperatures lead to faster crosslinking processes. As C=C bonds are not consumed during ageing,[3] the oxidation processes occurring during ageing are hindered at higher temperatures, because of the smaller number of oxidation sites. On the other hand, lower temperatures favor oxidation thanks to the slower crosslinking. In addition, ageing promotes changes in the surface morphology of EPDM at long periods, indicative of surface degradation. This could be related to migration of additives towards the surface as reflect the increase in Si or N XPS signals in the treatments at 100 days at both temperatures.

APPENDIX: NUMERICAL CALCULATION OF THE REAL SURFACE AREA AND THE ROUGHNESS RATIO

Real surface area of the samples was determined using approximate triangulation method from the matrix of points obtained by 3D surface scanning. The surface height was measured relative to a reference plane in $n \times m$ points forming a rectangular matrix. The points are equally spaced in each directions in the reference plane. For any point with indexes i and j, the coordinates in plane $x_{i,j}$, $y_{i,j}$ are given and the height $z_{i,j}$ is determined from the measurement. For each elementary matrix cell formed by four points with indexes (i, j), $(i + 1, j)$, $(i, j + 1)$, and $(i + 1, j + 1)$, the real surface was approximated by two triangles formed by the points with indexes (i, j), $(i + 1, j)$, and $(i, j + 1)$ for the first triangle and $(i + 1, j)$, $(i, j + 1)$, and $(i + 1, j + 1)$ for the second triangle.

The area of each triangle can be found from the Pythagorean sum of the areas of the respective projections on the three principal planes. For the first triangle:

$$S_{i,j,1} = \frac{1}{2}\sqrt{\left(\det\begin{bmatrix} x_{i,j} & x_{i+1,j} & x_{i,j+1} \\ Y_{i,j} & y_{i+1,j} & y_{i,j+1} \\ 1 & 1 & 1 \end{bmatrix}\right)^2 + \left(\det\begin{bmatrix} y_{i,j} & y_{i+1,j} & y_{i,j+1} \\ z_{i,j} & z_{i+1,j} & z_{i,j+1} \\ 1 & 1 & 1 \end{bmatrix}\right)^2 + \left(\det\begin{bmatrix} z_{i,j} & z_{i+1,j} & z_{i,j+1} \\ x_{i,j} & x_{i+1,j} & x_{i,j+1} \\ 1 & 1 & 1 \end{bmatrix}\right)^2} \quad \text{(A1)}$$

and for the second triangle:

$$S_{i,j,2} = \frac{1}{2}\sqrt{\left(\det\begin{bmatrix} x_{i+1,j+1} & x_{i+1,j} & x_{i,j+1} \\ y_{i+1,j+1} & y_{i+1,j} & y_{i,j+1} \\ 1 & 1 & 1 \end{bmatrix}\right)^2 + \left(\det\begin{bmatrix} y_{i+1,j+1} & y_{i+1,j} & y_{i,j+1} \\ z_{i+1,j+1} & z_{i+1,j} & z_{i,j+1} \\ 1 & 1 & 1 \end{bmatrix}\right)^2 + \left(\det\begin{bmatrix} z_{i+1,j+1} & z_{i+1,j} & z_{i,j+1} \\ x_{i+1,j+1} & x_{i+1,j} & x_{i,j+1} \\ 1 & 1 & 1 \end{bmatrix}\right)^2} \quad \text{(A2)}$$

Then, the total surface area is equal to the sum of the areas of all triangles:

$$S_{\text{tot}} = \sum_{i=1}^{n-1} \sum_{j=1}^{m-1} (S_{i,j,1} + S_{i,j,2}). \quad \text{(A3)}$$

The roughness ratio is calculated as follows:

$$r = S_{\text{tot}}/S, \quad \text{(A4)}$$

where

$$S = |(x_{n,1} - x_{1,1})(y_{1,m} - y_{1,1})|. \quad \text{(A5)}$$

A Matlab routine for the calculation of real surface area and the roughness ratio is available in the Supplementary materials of this article on the web site of the journal.

References

1. Gamlin, C. D.; Dutta, N. K.; Chouhury, N. R. Polym Degrad Stab 2003, 80, 525.
2. Majumder, P. S.; Bhowmick, A. K. Wear 1998, 221, 15.
3. Zhao, Q.; Li, X.; Gao, J. Polym Degrad Stab 2008, 93, 692.
4. Botros, S. H. Polym Degrad Stab 1998, 62, 471.
5. Delor-Jestin, F.; Lacoste, J.; Barrois-Oudin, N.; Cardinet, C.; Lemaire, J. Polym Degrad Stab 2000, 67, 469.
6. Kumar, A.; Commereuc, S.; Verney, V. Polym Degrad Stab 2004, 85, 751.
7. Gueguen, V.; Audouin, L.; Pinel, B.; Verdu, J. Polym Degrad Stab 1994, 43, 217.
8. Budrugeac, P.; Segal, E. Polym Degrad Stab 1994, 46, 203.
9. Grythe, K. F.; Hansen, F. K. Langmuir 2006, 22, 6109.
10. Navrátil, Z.; Bursikova, V.; Stáhel, P.; Sira, M.; Zverina, P. Czechoslovak J Phys 2004, 54, C887.
11. Gindl, M.; Sinn, G.; Gindl, W.; Reiterer, A.; Tschegg, S. Colloids Surf A: Physichochem Eng Asp 2001, 181, 279.
12. van Oss, C. J.; Good, R. J.; Chaudhury, M. K. Langmuir 1988, 4, 884.
13. Dilsiz, N.; Wightmann, J. P. Colloids Surf A: Physicochem Eng Asp 2000, 164, 325.
14. ISO/DIS 25178. Geometrical Product Specifications (GPS)—Surface Texture: Areal. ISO: Geneva, 2008.
15. Briggs, D.; Seah, M. P., Eds. Practical Surface Analysis, 2nd ed.; Auger and Photoelectron Spectroscopy. John Wiley & sons: New York, 1990; Vol. 1.
16. Beamson, G.; Briggs, D. High Resolution XPS of Organic Polymers. The Scienta ESCA300 Database. John Wiley & sons: New York, 1992.
17. Delor-Jestin, F.; Lacoste, J.; Barrois-Oudin, N.; Cardinet, C.; Lemaire, J. Polym Degrad Stab 2000, 67, 469.
18. Marmur, A. Langmuir 2003, 19, 8343.
19. Chow, T. S. J Phys Condens Matter 1998, 10, L445.
20. Ayala, J. A.; Rincón, M. E. ACS Fuel 1981, 26, 120.
21. Mason, L. R.; Reynolds, A. B. Polym Eng Sci 1998, 38, 1149.